
**Separation Science and Technology**
Publication details, including instructions for authors and subscription information:
http://www.informaworld.com/smpp/title~content=t713708471

# Preliminary Report on Ultrafiltration-Induced Polarization Chromatography—An Analog of Field-Flow Fractionation

H. L. Lee[a]; E. N. Lightfoot[a]
[a] Department of Chemical Engineering, University of Wisconsin, Madison, Wisconsin

**To cite this Article** Lee, H. L. and Lightfoot, E. N.(1976) 'Preliminary Report on Ultrafiltration-Induced Polarization Chromatography—An Analog of Field-Flow Fractionation', Separation Science and Technology, 11: 5, 417 — 440
**To link to this Article: DOI:** 10.1080/01496397608085333
**URL:** http://dx.doi.org/10.1080/01496397608085333

SEPARATION SCIENCE, 11(5), pp. 417–440, 1976

# Preliminary Report on Ultrafiltration-Induced Polarization Chromatography—An Analog of Field-Flow Fractionation

H. L. LEE and E. N. LIGHTFOOT

DEPARTMENT OF CHEMICAL ENGINEERING
UNIVERSITY OF WISCONSIN
MADISON, WISCONSIN 53706



**Abstract**

Ultrafiltration-induced polarization chromatography (UPC), belonging to the class of field-flow fractionations, is examined in some depth mathematically, and predictions based on this examination are tested against preliminary experimental data. Both analysis and experiments are performed for slit flow between porous confining walls with a superimposed cross flow perpendicular to these walls. Integration of the diffusion equation for an idealized two-dimensional flow suggests that UPC is a very promising alternate to gel permeation chromatography, both for determining polymer diffusion coefficients and estimating the molecular-weight distribution of mixtures. These predictions are borne out to a substantial degree by experiments with monodisperse native proteins, but it is clear that important practical problems remain to be solved. The most important of these are adsorption of protein and deviation of flow distribution from that modeled.

## INTRODUCTION

It has been increasingly recognized that selective dynamic polarization is an attractive alternate to partial sorption in an immobilized phase for producing the solute distributions needed in countercurrent separations. The oldest examples of this type appear to be electrodecantation (*1*), countercurrent separations by thermal diffusion (*2*), and electrophoresis (*3*, *4*). More recently polarization techniques have been proposed for a

variety of chromatographic separations: the field-flow fractionations of Giddings and his colleagues* (*5*) or the single-phase chromatography of Lee et al. (*6*) and Reis and Lightfoot (*14*). We refer to these latter here under the general heading of *polarization chromatography* and concentrate our attention on ultrafiltration-induced polarization chromatography (UPC).

Such a process is illustrated in Fig. 1 for a slit-flow apparatus in which polarization is provided at one lateral surface by a cross flow perpendicular to the main (axial) flow. This cross flow concentrates solutes to be separated into the slow-moving fluid near the polarizing wall and thus retards their progress in the primary flow direction. Separation of solute pulses results from differences in their degrees of segregation, primarily resulting from differences in their effective binary diffusivities relative to the solvent. Normally the solutes of interest are fed as short pulses at the column inlet just as in more conventional chromatographic operations.



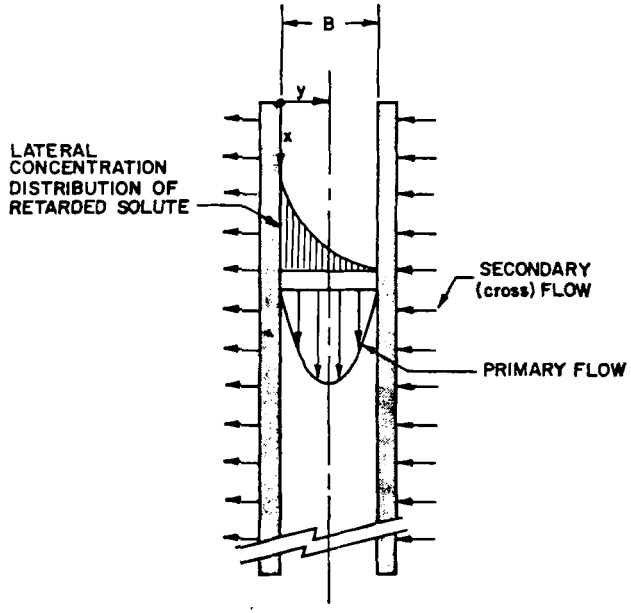


FIG. 1. Velocity and concentration profiles in UPC.

*A manuscript paralleling our paper by Giddings, Yang, and Myers is currently under review.

UPC has already been suggested by Lee et al. (*6*) as a means of polymer fractionation and for the estimation of molecular-weight distributions of polymeric mixtures. For both of these applications it offers the advantages of short response times, small axial dispersion, and good reproducibility; all these are characteristic of polarization chromatography in general, and they are discussed in some detail below. In addition, use of ultrafiltration to produce polarization offers the specific advantages of general applicability and primary dependence on a single well-defined property, the mass diffusivity $\mathscr{D}_{is}$.

UPC does, however, suffer from two specific disadvantages: loss of solvent through the active boundary and the development of finite osmotic pressures at this boundary. In addition it can, of course, be seriously affected by adsorption phenomena or irreversible solute precipitation.

It has already been shown by Lee et al. (*6*) that solvent loss is a severe problem in the tubular geometry used by them and is likely to require the use of very large-diameter tubes. This appears at present to be a severe problem, and for this reason we currently prefer the slit-flow arrangement of Fig. 1. However, we shall see below that even here the need to maintain simultaneous control of the primary and cross flows presents practical problems not yet entirely solved.

The characteristically sharp increase of polymer osmotic pressure with concentration may also be troublesome, because it tends to decrease the polarizing cross flow most strongly in the concentrated regions of the solute pulses. This in turn tends to broaden the pulse. Such broadening can be minimized either by keeping solute concentrations low or by using membranes of very low hydraulic permeability, but in any event it must be considered.

Our approach here is to begin by developing a quantitative a priori description of UPC for an idealized two-dimensional flow situation and then to test the utility of this description by preliminary experiments with well-defined solutes. We shall see that both the theoretical analysis and experimental verification are encouraging, but all of the above-mentioned problems are in fact found to be important.

## THEORY

We consider here what happens when a small solute pulse is introduced to the flow channel of Fig. 1, and we confine our attention for the moment to a somewhat idealized situation: we assume steady two-dimensional laminar flow and pseudobinary diffusion. Solute motion is then described

by:

$$\frac{\partial c}{\partial t} + \frac{\partial}{\partial x} cv_x + \frac{\partial}{\partial y} cv_y = \mathscr{D}\left(\frac{\partial^2 c}{\partial x^2} + \frac{\partial^2 c}{\partial y^2}\right) \tag{1}$$

Here $c$ is concentration of the polymeric solute under consideration, $\mathscr{D}$ is an effective binary diffusivity of this solute, and $v$ is the fluid velocity. System geometry is defined in Fig. 1. We next assume the cross-flow velocity to be small compared to the axial-flow velocity, and that the effects of polymer concentration on system hydrodynamics are negligible. The velocity profile is then described by

$$v_x = 6\bar{u}\left[\left(\frac{y}{B}\right) - \left(\frac{y}{B}\right)^2\right] \tag{2}$$

$$v_y = -v_w \tag{3}$$

Here $\bar{u}$ is the flow-average axial velocity, and $v_w$ is the velocity of the cross flow; both are considered constant. We shall consider more complex flow patterns later.

The boundary conditions on concentration are obtained from the assumption that solute cannot penetrate the walls. Thus

$$v_y c = \mathscr{D}\frac{\partial c}{\partial y} \qquad \text{at} \quad y = 0, B \tag{4}$$

This is normally a good approximation.

Equation (1) can be averaged formally over the channel width with the aid of Eq. (4) to obtain

$$\frac{\partial \langle c \rangle}{\partial t} + \frac{\partial}{\partial x}\langle v_x c \rangle = \mathscr{D}\frac{\partial^2 \langle c \rangle}{\partial x^2} \tag{5}$$

where

$$\langle Q \rangle \equiv \frac{1}{B}\int_0^B Q\, dy \tag{6}$$

Henceforth $\langle c \rangle$ will be written as $c_m$, the area *mean* concentration. It is our purpose to determine $c_m$ as a function of position and time, and we shall do this by obtaining useful explicit approximations for $\langle v_x c \rangle$ in terms of the mean velocity $\bar{u}$ and mean concentration $c_m$.

To do this we follow the lead of Gill et al. (*11*) and postulate that

$$c = \sum_{k=0}^{\infty} f_k(y, t)\frac{\partial^k c_m}{\partial x^k} \tag{7}$$

Putting Eq. (7) into Eq. (5) we get

$$\frac{\partial c_m}{\partial t} + \langle v_x f_0 \rangle \frac{\partial c_m}{\partial x} = (\mathscr{D} - \langle v_x f_1 \rangle)\frac{\partial^2 c_m}{\partial x^2} - \sum_{k=2}^{\infty} \langle v_x f_k \rangle \frac{\partial^k c_m}{\partial x^k} \tag{8}$$

or

$$\frac{\partial c_m}{\partial t} + R\bar{u}\frac{\partial c_m}{\partial x} = (\mathscr{D} + \varepsilon)\frac{\partial^2 c_m}{\partial x^2} - \sum_{k=2}^{\infty} \langle v_x f_k \rangle \frac{\partial^k c_m}{\partial x^k} \tag{9}$$

where

$$R \equiv \langle v_x f_0 \rangle / \bar{u} \tag{10}$$

and

$$\varepsilon = -\langle v_x f_1 \rangle \tag{11}$$

Equation (9) is convenient for our purposes because $R$ and $\varepsilon$, from the first two terms of Eq. (7), have particularly important physical significance: the *retardation factor* $R$ is just the ratio of the mean convective velocity of solute to that of solvent, while $\varepsilon$ is an *effective axial dispersion coefficient*, resulting from the equivalent of Taylor dispersion in this system. The remaining terms of the series are needed to provide detailed descriptions of pulse shape, but they are of secondary importance, particularly in long columns. Our primary objective is then to obtain predictions of $R$ and $\varepsilon$, which are functions only of time, and our secondary objective is to obtain expressions for the higher terms $\langle v_x f_k \rangle$.

To achieve these objectives we must obtain differential equations for the individual $f_k$; to do this we put Eq. (7) into Eq. (1) and eliminate $\partial c_m/\partial t$ through use of Eq. (5). The result may be expressed as:*

$$\sum_{k=0}^{\infty}\left[\frac{\partial f_k}{\partial t} + f_{k-1}v_x - \frac{\partial f_k}{\partial y}v_w - \mathscr{D}\frac{\partial^2 f_k}{\partial y^2}\right]\frac{\partial^k c_m}{\partial x^k} = \sum_{j=0}^{\infty}\sum_{k=0}^{\infty} f_k \langle v_x f_j \rangle \frac{\partial^{j+k+1} c_m}{\partial x^{j+k+1}} \tag{12}$$

We now equate coefficients of each $\partial^k c_m/\partial x^k$ to obtain

$$\frac{\partial f_k}{\partial t} + f_{k-1}v_x - \frac{\partial f_k}{\partial y}v_w - \mathscr{D}\frac{\partial^2 f_k}{\partial y^2} = \sum_{i=0}^{k-1} f_i \langle v_x f_{k-1-i} \rangle \tag{13}$$

with the boundary conditions

$$\mathscr{D}\frac{\partial f_k}{\partial y} + v_w f_k = 0 \qquad \text{at} \quad y = 0, B \tag{14}$$

*All $f_k$ for $k < 0$ are defined to be zero.

Equations (13) and (14) give a description for each $f_k$ in terms of those with smaller index.

Note that Eq. (7) requires

$$\langle f_k \rangle = 1 \qquad \text{for} \quad k = 0 \tag{15}$$

$$\langle f_k \rangle = 0 \qquad \text{for} \quad k > 0 \tag{16}$$

It is clear that Eq. (13) is consistent with these requirements.

We next rewrite Eqs. (13) and (14) in terms of the dimensionless quantities

$$\eta = y/B$$

$$\alpha = 6\bar{u}/v_w$$

$$\phi_k = f_k/B^k$$

$$\tau = tv_w/B$$

$$\text{Pé} = Bv_w/\mathscr{D}$$

We thus obtain

$$\frac{\partial \phi_k}{\partial \tau} + \alpha(\eta - \eta^2)\phi_{k-1} - \frac{\partial \phi_k}{\partial \eta} - \frac{1}{\text{Pé}} \frac{\partial^2 \phi_k}{\partial \eta^2} = \sum_{i=0}^{k-1} \alpha \phi_i \langle (\eta - \eta^2)\phi_{k-1-i} \rangle \tag{17}$$

$$\frac{\partial \phi_k}{\partial \eta} + \text{Pé}\phi_k = 0 \qquad \text{at} \quad \eta = 0, 1 \tag{18}$$

which completes the formal statement of our problem.

Now according to the Sturm-Liouville theorem eigenfunctions of the operator

$$\frac{1}{\text{Pé}} \frac{d^2}{d\eta^2} + \frac{d}{d\eta}$$

which satisfy Eq. (18) are orthogonal over the interval ($0 \leqslant \eta \leqslant 1$) with respect to the weighting function $\exp[\text{Pé}\eta]$. We may therefore expand each $\phi_k$ in a series of these eigenfunctions, denoted as $Y_n(\eta)$, in the form

$$\phi_k = \sum_n T_{kn}(\tau) Y_n(\eta) \tag{19}$$

Any such expression will automatically satisfy Eq. (18).

Substitution of Eq. (19) into Eq. (17) gives

$$\sum_n \left[ \frac{dT_{kn}}{d\tau} + \lambda_n T_{kn} \right] Y_n = \alpha \left[ \sum_{i=0}^{k-1} \phi_i F_{k-1-i} - (\eta - \eta^2)\phi_{k-1} \right] \tag{20}$$

where

$$F_k = \langle(\eta - \eta^2)\phi_k\rangle$$

and $-\lambda_n$ is the eigenvalue for the eigenfunction $Y_n$.

We now multiply each side of Eq. (20) by $Y_m e^{\mathrm{P\acute{e}}\eta}$ and integrate with respect to $\eta$ over the interval ($0 \leqslant \eta \leqslant 1$). We thus obtain:

$$\frac{dT_{km}}{d\tau} + \lambda_m T_{km} = \alpha\left\langle\left[\sum_{i=0}^{k-1}\phi_i F_{k-1-i} - (\eta - \eta^2)\phi_{k-1}\right]e^{\mathrm{P\acute{e}}\eta}Y_m\right\rangle \quad (21)$$

This result may be immediately integrated to give

$$T_{kn}(\tau) = e^{-\lambda_n\tau}\left\{\alpha\int_0^\tau e^{\lambda_n\tau}\left\langle\left[\sum_{i=0}^{k-1}\phi_i F_{k-1-i} - (\eta - \eta^2)\phi_{k-1}\right]e^{\mathrm{P\acute{e}}\eta}Y_n\right\rangle d\tau + T_{kn}(0)\right\} \quad (22)$$

Equation (22) provides the basis for determining all the $f_k$.

Our primary interest is, however, in $\phi_0$ and $\phi_1$, and we now confine our interest to these. The summation in Eq. (17) then simplifies to

$$\sum_{i=0}^{k-1}\alpha\phi_i\langle(\eta - \eta^2)\phi_{k-1}\rangle = 0 \qquad (k = 0) \quad (23)$$

$$= \alpha\phi_0\langle(\eta - \eta^2)\phi_0\rangle \qquad (k = 1) \quad (24)$$

In addition, $\phi_{k-1} = 0$ for $k = 0$. We thus find

$$\frac{\partial\phi_0}{\partial\tau} - \frac{\partial\phi_0}{\partial\eta} - \frac{1}{\mathrm{P\acute{e}}}\frac{\partial^2\phi_0}{\partial\eta^2} = 0 \quad (25)$$

$$\frac{\partial\phi_1}{\partial\tau} - \frac{\partial\phi_1}{\partial\eta} - \frac{1}{\mathrm{P\acute{e}}}\frac{\partial^2\phi_1}{\partial\eta^2} = \alpha\phi_0[\langle(\eta - \eta^2)\phi_0\rangle - (\eta - \eta^2)] \quad (26)$$

These equations are to be integrated with the aid of Eq. (18) and the initial conditions

$$\phi_0(0, \eta) = 1 \qquad (0 < \eta < 1) \quad (27)$$

$$\phi_1(0, \eta) = 0 \qquad (0 < \eta < 1) \quad (28)$$

Equations (27) and (28) are true for solute initially distributed uniformly over the flow cross section.

This process is particularly simple for $\phi_0$ and leads to

$$\phi_0 = \phi_0^{(\infty)} + \phi_0^{(t)} \quad (29)$$

where

$$\phi_0^{(\infty)} = \text{Pé}\, e^{-\text{Pé}\eta}/(1 - e^{-\text{Pé}}) \tag{30}$$

and

$$\phi_0^{(t)} = \sum_{n=1}^{\infty} T_{0n}(\tau)\, Y_n(\eta) \tag{31}$$

where

$$T_{0n}(\tau) = \frac{(e^{\text{Pé}/2}(-1)^n - 1)\text{Pé}}{[n^2\pi^2 + (\text{Pé}/2)^2]} \exp - \left[\text{Pé} + \frac{4n^2\pi^2}{\text{Pé}}\right]\frac{\tau}{4} \tag{32}$$

$$Y_n(\eta) = \frac{e^{-\text{Pé}\eta/2}[n^2\pi^2 \cos n\pi\eta - (n\pi\text{Pé}/2) \sin n\pi\eta]}{[n^2\pi^2 + (\text{Pé}/2)^2]} \tag{33}$$

Note that $\phi_0$ depends only upon one parameter, the Péclet number. We shall see later that the transient contribution normally decays rapidly enough to be of negligible practical importance.

## PREDICTED BEHAVIOR

We now use the above theory to explore the utility of UPC as a separations tool. To do this without undue mathematical difficulty we truncate Eq. (8) to yield an approximate but useful description which can be compared directly to those used for describing presently available alternate processes. In this way we show that UPC is sufficiently attractive to justify a substantial developmental effort.

We begin by eliminating all derivatives of order higher than 2 in Eq. (8) to obtain:

$$\frac{\partial c_m}{\partial t} + R(t)\bar{u}\frac{\partial c_m}{\partial x} \doteq [\mathscr{D} + \varepsilon(t)]\frac{\partial^2 c_m}{\partial x^2} \tag{34}$$

where

$$R(t) = \langle v_x f_0\rangle/\bar{u} = 6\langle(\eta - \eta^2)\phi_0\rangle \tag{35}$$

and

$$\varepsilon(t) = -\langle v_x f_1\rangle = -B\bar{u}6\langle(\eta - \eta^2)\phi_1\rangle \tag{36}$$

Equation (34) is just the one-dimensional diffusion equation, with time-dependent convection and dispersion as described by Eqs. (35) and (36). It is identical in form to the equations used most commonly for describing

alternative chromatographic processes and is therefore ideally suited for comparison purposes. It is probably also of acceptable accuracy.

Essentially all linear chromatographic processes can be adequately described by Eq. (34) if $R$ and $\varepsilon$ are properly chosen. This is always true in sufficiently long columns [see, for example, Giddings (*7*)], but it is usually reasonable even in rather short ones. More specifically, $R$ and $(\mathscr{D} + \varepsilon)$ are normally adequate to describe, respectively, the first and second moments of concentration with respect to axial position. We shall therefore concentrate on these two quantities.*

We begin with $R$ which at any time represents the ratio of mean solute to solvent velocities in the axial direction. We begin by noting that for large times

$$R \doteq 6\langle(\eta - \eta^2)\phi_0^{(\infty)}\rangle = (6/\text{Pé})\left[\coth\left(\frac{\text{Pé}}{2}\right) - \frac{2}{\text{Pé}}\right] \tag{37}$$

This result is plotted in Fig. 2, and shows that good separability is achieved

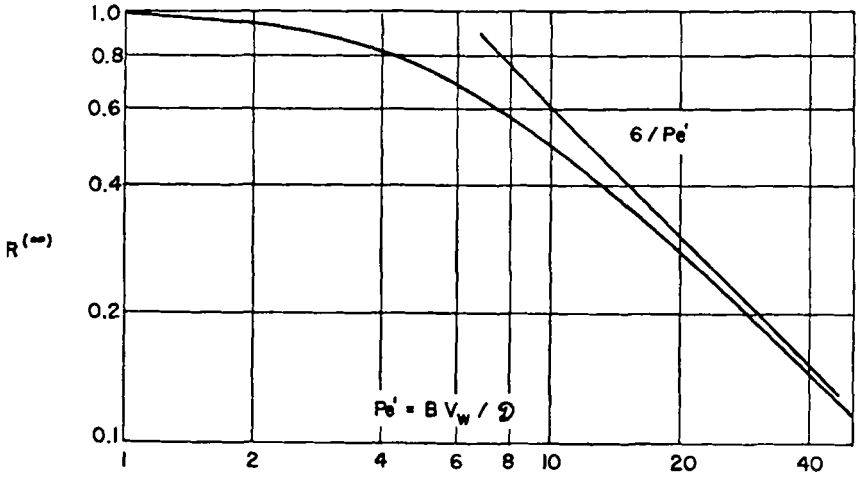


FIG. 2. Retardation factors as a function of Péclet number.

*It is, however, necessary to keep higher terms to describe skewness, and more particularly the bimodal peaks noted by Lee et al. (*6*) for small $\tau$. A more efficient computational scheme is now under development for such short-time behavior.

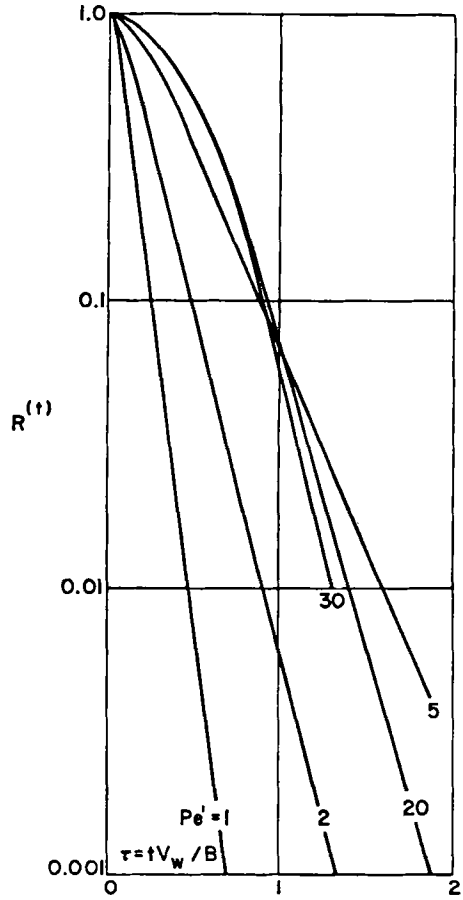


FIG. 3. Transient contributions to the retardation factor.

for Pé greater than about 10. In this region solute holdup time is approximately proportional to the Péclet number. One must, however, also consider the effect of transients since at zero time $R$ is unity for all Péclet numbers. The decay of the transient contribution is shown in Fig. 3, and it can be seen here that this decay is rapid. Even under the worst situation (Péclet numbers near 5), 90% of the transient effect is eliminated by $\tau$ equal to unity: the time required for convection across the slit.* Furthermore, for Pé greater than about 30 the fractional decay rate is fast and essentially independent of Pé. If transients are a problem, one can always permit a solute pulse to redistribute before permitting an axial flow. This procedure has been successfully tested by Lee et al. (*6*).

It appears then that separations comparable to gel permeation chromatography can be achieved if it proves possible to operate at Péclet numbers of about 10 to $10^2$. It should also be noted that UPC is potentially much more flexible than GPC since the retardation of any high molecular-weight species may be changed simply by adjusting the cross flow.

We next turn our attention to the effective axial dispersion coefficient $\varepsilon(t)$ and again consider first the long-time asymptotic behavior. In Fig. 4 are plotted values of $(\varepsilon(\infty)/B^2\bar{u}^2)\mathscr{D}$ as a function of Pé. This ordinate is chosen because for a Péclet number of zero the effective axial dispersion coefficient is (*9*):

$$\underset{\substack{t\to\infty \\ \text{Pé}\to 0}}{\text{Limit}}\{\varepsilon\} = \frac{B^2\bar{u}^2}{210\mathscr{D}} \tag{38}$$

This limiting result, for *Taylor dispersion*, is also plotted in the figure as a horizontal dotted line.

Figure 4 shows that the dispersion coefficient is at first larger than the Taylor limit and then much smaller, as the Péclet number increases. From a practical standpoint this is in accord with the retardation behavior in suggesting operation at Péclet numbers above about 10 to 20: for Pé larger than these, axial dispersion becomes very small indeed and separation correspondingly sharp. In fact, the sharp drop of axial dispersion with increasing Péclet number is one of the most attractive features of this separation technique. This predicted performance is far superior to anything possible with packed beds for particle sizes comparable to $B$. It may be seen from Fig. 5 that the dispersion transients die out in about the same

*Note that if $v_w$ and $\bar{u}$ are of the same order of magnitude, the mean dimensionless residence time for the solute $\bar{\tau} \sim (L/BR_f)$, where $L$ is the column length. Normally $\bar{\tau} \gg 1$ for the large Pé where transients are most harmful.

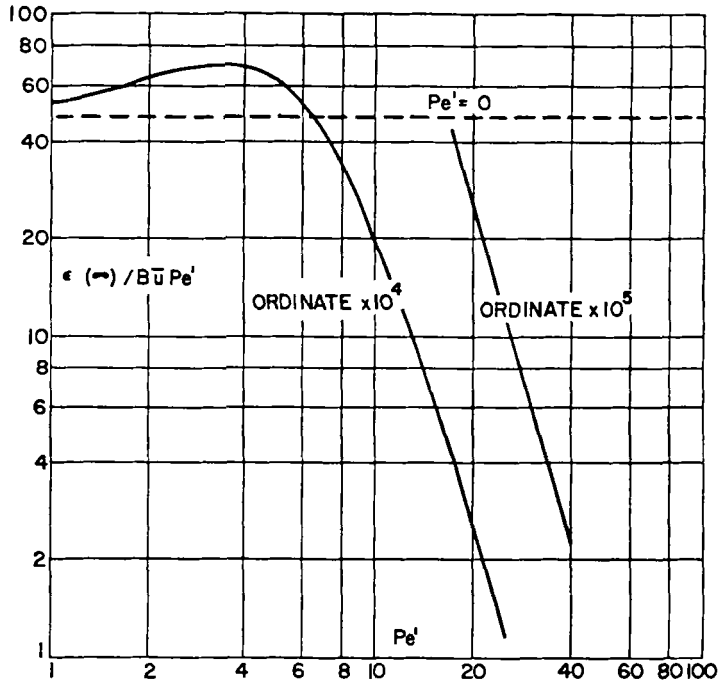


FIG. 4. Asymptotic axial dispersion as a function of Péclet number.

time as the transient contributions to $R$. This is to be expected, but it shows that transients are of interest for the high Péclet numbers needed for effective separation: much of the observed dispersion may take place in the transient region even though it is short compared to species retention time.

The complex dependence of the asymptotic dispersion coefficients on Péclet number is not immediately obvious and is perhaps worth a short digression.

It is clear that the observed dispersion of a solute pulse represents a nonuniform distribution of residence times, and a little thought suggests that it results from a balance of two opposing factors: dispersion results from the nonuniformity of the velocity profile $v_x(y)$, and it is mitigated by the tendency of solute particles to move randomly in the $y$-direction. Now as the solute is compressed into an ever smaller boundary layer near $y = 0$,

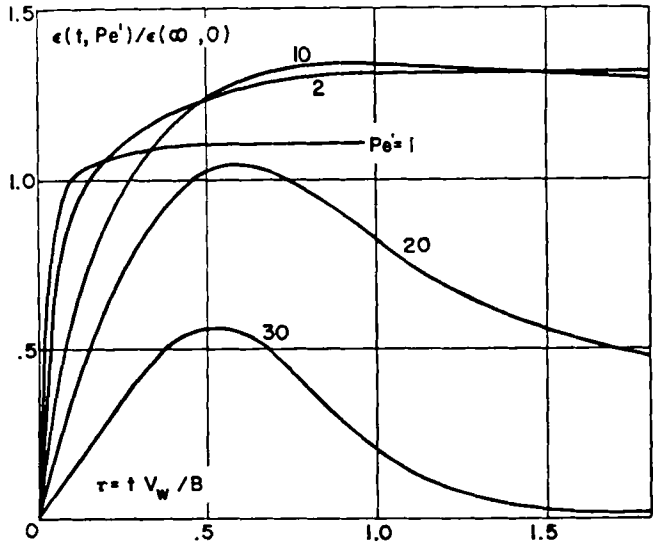


FIG. 5. Effect of time and Péclet number on axial dispersion.

these two factors change in relative importance. The effective nonuniformity of the velocity profile becomes more pronounced as the linear profile near the wall becomes more important. This tends to increase dispersion and is the dominant factor for small Péclet number. However, as the boundary layer becomes thinner, redistribution of solute in the $y$-direction occurs more rapidly. This effect tends to decrease dispersion, and it is dominant for the higher Pé. In fact, once the velocity profile is effectively linear throughout the boundary layer, the distribution of axial velocities is Pé independent, and a simple boundary-layer analysis suffices to characterize dispersion. In this region

$$\varepsilon = \frac{72}{\text{Pé}^4}\frac{B^2\bar{u}^2}{\mathscr{D}} \tag{39}$$

This actually was the result obtained by Giddings for his analysis of thermal field-flow fractionation in a thin rectangular channel (*8*). As our calculation shows, this limit is reached only at impracticably large Péclet number.

## EXPERIMENTAL VERIFICATION

The above predictions were tested experimentally in the prototype apparatus shown in Figs. 6 through 8 using both native proteins and synthetic dextrans.

### Apparatus and Procedure

A slit-flow apparatus is constructed to provide the flow pattern in Fig. 1. Its actual design is shown in Fig. 2, and consists essentially of a rectangular channel formed by sandwiching a spacer between two porous rectangular plates. The spacer is simply a thin sheet of metal or plastic with perforations as shown in Fig. 7. The thickness of the spacer varies, and for our experiments two values, 0.1 and 0.033 cm, have been used. These values turned out to be extremely critical, and determined to a great extent the composition of the upper wall of the channel. With a 0.1-cm spacer, a stainless steel sintered plate (Pall Trinity Corp.) is sufficient for the upper wall. The permeability of the sintered plate is

$$\frac{1.494 \times 10^{-1} \text{ cm/sec}}{1 \text{ psi}}$$

or $2.167 \times 10^{-6}$ cm$^3$/dyne-sec. This gives a maximum variation of 0.5% in $\bar{u}$, and is therefore quite satisfactory. With a 0.033-cm spacing, the maximum variation becomes 13%. A membrane is now needed for the upper wall, and it is sandwiched between two porous plates for mechanical stability. It is important to have a sintered metal plate below the membrane, since metal plates are more rigid and less porous than plastic. For the lower wall a membrane is always needed, and it is layered on top of a porous polyethylene plate.

The porous plates are further embedded in two blocks of aluminum which provide mechanical strength and also inlet and outlet connections for the solvent flows. The slabs are then clamped together by screws through slots drilled on both of their sides.

The slit-flow apparatus forms the core of the experimental setup, shown in Fig. 8. A Cole-Parmer variable speed centrifugal pump is used to deliver the cross flow, which is first passed through a filter to remove any large-size contaminants. Otherwise the particles will accumulate within the slit-flow apparatus. The direct flow into the slit is supplied by a syringe pump (Harvard Apparatus) which is capable of delivering steady, pulseless flow. Solvent which has not passed through the lower membrane leaves at the

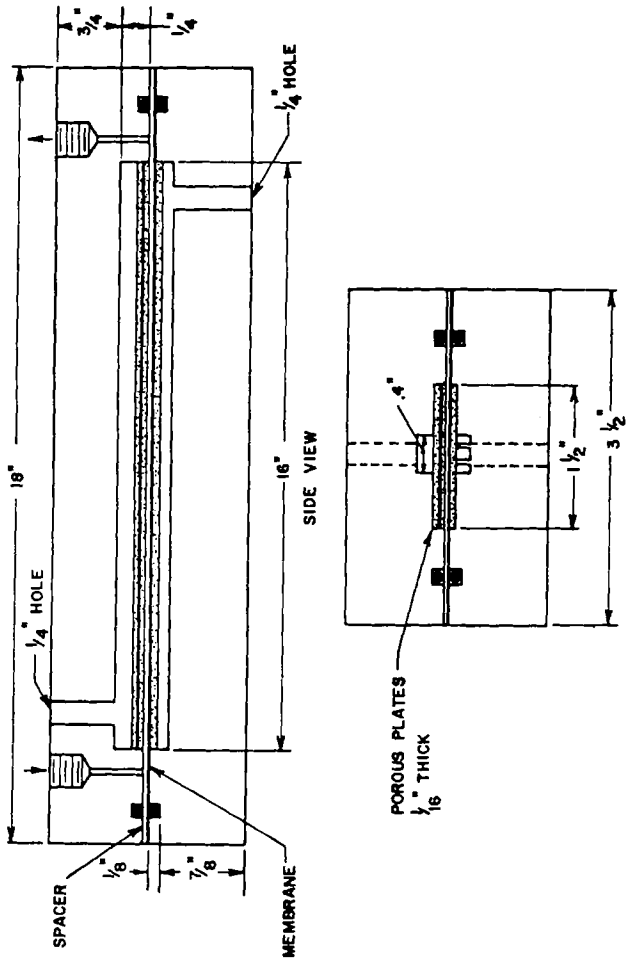


FIG. 6. Slit-flow apparatus.

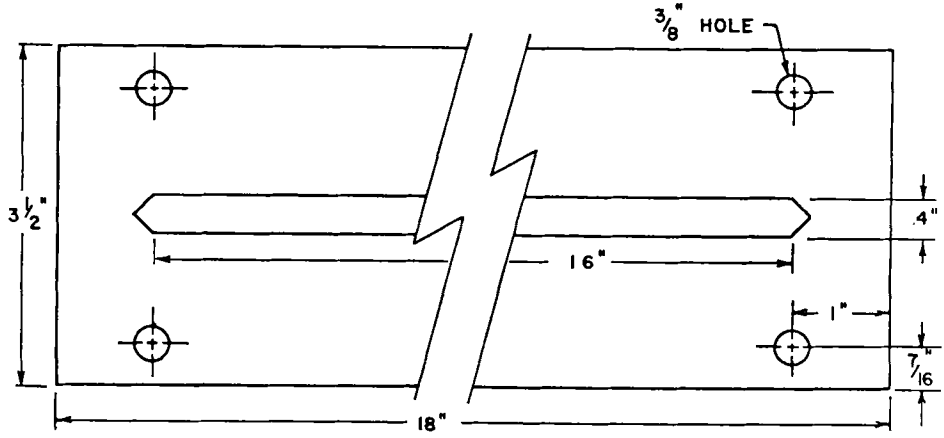


FIG. 7. Top view of spacer. There are five 0.95 cm holes on each side, spaced 10.2 cm apart

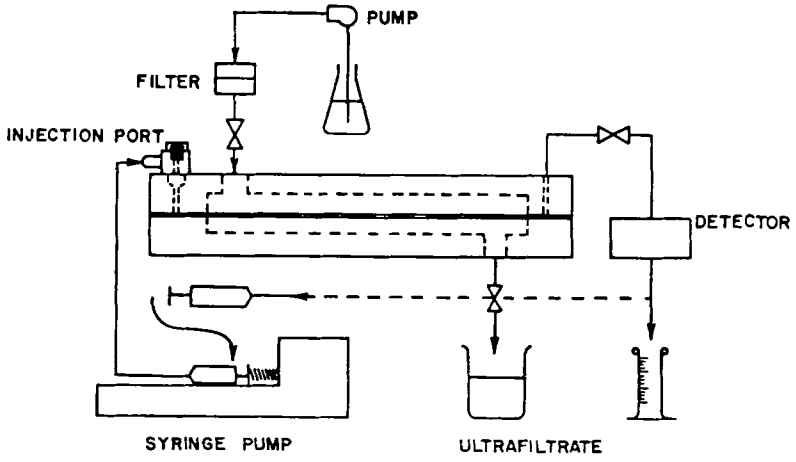


FIG. 8. Experimental setup for UPC.

end of the slit, and is then passed through a valve into the detector. From the detector it also has the option of going into a syringe, withdrawing at a constant rate, or simply a container.

The boundary condition that $\bar{u}$ is the same at the inlet and outlet of the channel can be achieved by either one of two means: First with the valves for the cross flow shut off, the flow rate through the detector is measured at a known syringe pump speed. This flow rate is reproduced as precisely as possible for runs with cross flow by adjusting the valves at the outlets of the apparatus. The reproducibility, however, is normally within 10% only. Better control can be obtained if a syringe pump is used to withdraw solvent from the slit exit. However, this backs up a fluid pressure in the detector's flow cell, and since the pressure within the equipment fluctuates, the detector must be insensitive to pressure. When a differential refractometer (Waters Assoc.) is used, since it is very sensitive to pressure, withdrawal by a syringe pump causes a fluctuating base line, which is undesirable.



## Practical Implementation

Ultrafiltration polarization chromatography requires first the establishment of the ideal flow configuration as already described. Macromolecules, once introduced into the channel through the injection port (Fig. 4), are convected along the channel as well as toward the lower wall. A membrane must be present at the lower wall to retain the solutes in the channel. Ideally the membranes, as well as the upper wall, are totally inert to the macromolecules. In practice, since a membrane is needed at the upper wall to ensure uniform distribution of cross flow, it must be supported from below by a stiff porous plate. It is difficult to find a porous plate made with materials inert to proteins. Polyethylene adsorbs proteins, and is also not sufficiently rigid to support the membrane. A sintered stainless steel plate (Pall-Trinity Corp.) is therefore used, since it has the advantage of rigidity and low porosity.

The experimental procedure consists simply of the following. The flow rates at the inlet and outlet of the rectangular channel were first adjusted equal, at least approximately, by the procedure just described. A small volume of a solution of macromolecules was then introduced with a syringe through the injection port on the separation equipment (Fig. 8). The solvent flow rate through the lower wall of the channel was measured by recording the time taken to collect 0.8 cc of permeate. The outlet flow

rates from the channel were found to vary during each run, but valve adjustment was avoided as it might introduce gas bubbles into the detector.

Solute was normally fed at 1/2% concentration by weight of macromolecular material. This is the minimum recommended for the detector which was a Waters differential refractometer.

Bovine serum albumin (BSA) was used in most of the experiments reported as it is a readily available, well-characterized monodisperse molecule. A few experiments were also made with polydisperse dextrans, and attempts were made to use a variety of other native proteins. Most of these latter tended to adsorb or precipitate irreversibly in the equipment, however.

Data were always obtained as refractive index of column effluent vs time. However, it was confirmed that the peaks observed were due to protein by ninhydrin test.

Two types of membranes were used, the PM and UM series of Amicon Corp., and both had a molecular weight cutoff below 5000, sufficient to retain all macromolecules used.



## Experimental Results and Interpretation

### *Retardation*

The first membrane tested, type UM2, gave very satisfactory results, which are summarized in Fig. 9. Shown here are experimental values of the retardation factor $R$ as a function of Péclet number. The solid line in the figure represents the theoretical prediction (same as Fig. 5). These

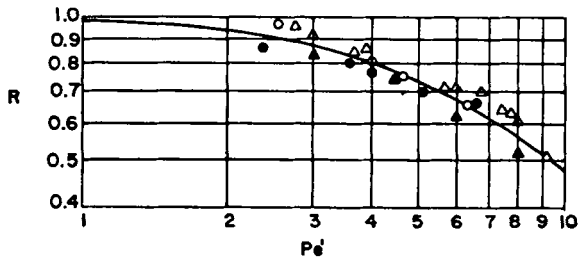


FIG. 9. Comparison of observed retardation with prediction ($B = 0.033$ cm): (△, ○) $\bar{u} \doteq 2.3$ cm/sec; (▲, ●) $\bar{u} \doteq 1.15$ cm/sec; (○, ●) "new" membranes; (△, ▲) "old" membranes.

results were obtained using a 0.01 $M$ Tris-base buffer adjusted to pH 8.5 with hydrochloric acid.

Retardation factors were calculated from the formula

$$R = \frac{\text{volume of channel/flow rate at inlet}}{\text{retention time of observed peak}} \tag{40}$$

which is correct if $\bar{u}$ is constant along the flow channel. The Péclet number was calculated from

$$\text{Pé} = \frac{(\text{cross-flow rate/open area})(\text{spacer thickness})}{\mathscr{D}} \tag{41}$$

The diffusivity of BSA was assumed to be $5.9 \times 10^{-7}$ cm$^2$/sec, the value recommended by Tanford (*10*) for infinite dilution. For all runs reported in Fig. 9 the spacer thickness was 0.033 cm.

The solid symbols in the figure represent data taken at axial flow rates of 0.0382 ml/min ($\bar{u} \doteq 1.15$ cm/min) and the hollow symbols data at 0.0764 ml/min ($\bar{u} \doteq 2.3$ cm/min).

The average of the data is clearly indistinguishable from the theoretical prediction, but there is a noticeable effect of axial flow rate not predicted by the theory. This difference most probably reflects calculation of retention time from the position of the peak in the effluent curve rather than that of the center of mass. All peaks exhibit some "tailing," so $R$ should be lower than indicated in Fig. 9, and the tailing was more severe at the higher flow rates. This asymmetry in turn is not calculable from our theory which is limited in effect to first and second moments of concentration.

It may be noted that we do not yet have reliable retardation data for Péclet numbers above 10, which is the most interesting region. In addition we are still encountering difficulties in the lower range of Pé, presumably because of inadequate flow control.

Thus retardation with a typical PM5 membrane was initially greater than predicted but soon became less. More specifically, we believe we are observing nonuniform membrane fouling as a result of protein deposition and consequent nonuniform cross flow.

*Dispersion*

The distribution of solute about the mean elution time was examined by comparing observed elution curves with the integrated form of Eq. (34),

which has the form

$$c_m = c_0/\sqrt{t}\, \exp\left[-(x - R\bar{u}t)^2/4(\mathscr{D} + \varepsilon)t\right] \tag{42}$$

where $c_0$ is a normalization constant. To facilitate comparison, the maximum of $c_m$ was chosen to coincide with that of observed peak. However, $R$ and $\varepsilon$ were calculated directly from the theory, using the large-time asymptotic values. This neglect of transients is reasonable since mean solute retention times $\bar{t}$ were normally much larger than $B/v_w$. For the situation shown in Fig. 10, for example, $\bar{t} = 21.4$ min and $B/v_w = 7.7$ min. Then $\bar{\tau} \sim 2.8$, and it can be seen from Figs. 3 and 5 that transients should not be of primary importance.

In general, the calculated and observed degrees of dispersion are quite close, as shown for two typical runs in Figs. 10 and 11. At low cross flows, as in Fig. 10, peak width was usually a bit less than predicted, while at higher cross flows, as in Fig. 11—or for lower axial flows—it was normally

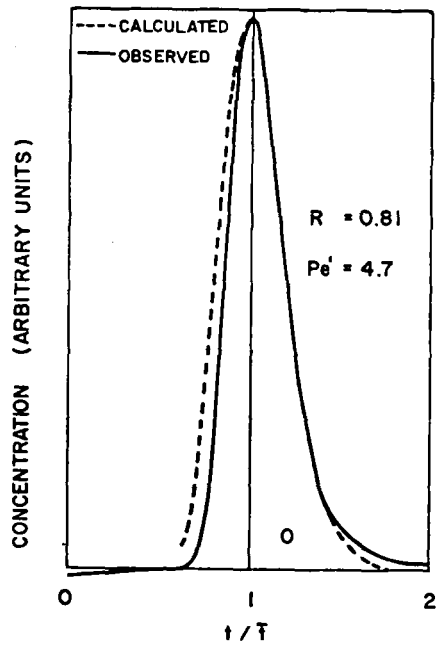


FIG. 10. Comparison of observed and predicted dispersion of BSA solution at 0.0764 ml/min. Mean solute retention time = $\bar{t}$ = 21.4 min. Solvent retention time = 17.25 min.

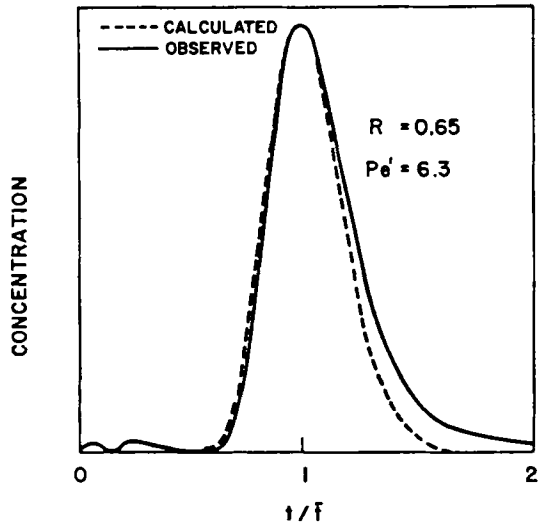


FIG. 11. Comparison of observed and predicted dispersion of BSA solution at 0.0764 ml/min. Mean solution retention time = $\bar{t}$ = 26.14 min. Solvent retention time = 17.25 min.

a bit broader. There is also appreciable tailing in all cases, and it would be desirable to extend the theory to determine whether this is unavoidable or due to defects in the procedure used.

Figures 10 and 11, and our remaining data, do indicate essential agreement with the two-parameter theory used for prediction, but they do not constitute a definitive test. All of our data were taken in the range ($2 <$ Pé $< 10$) over which $\varepsilon$ does not depart significantly from the Taylor limit (for Pé = 0). The very low dispersions predicted for higher Péclet numbers remain to be tested.

*Protein Recovery*

In all cases protein recovery was less than quantitative, and losses increased with retardation. For example, in representative results 32% of BSA was lost at $R = 0.7$ and 80% at 0.25. It was for this reason that it was not feasible to use high Péclet numbers in these preliminary tests.

We have as yet no evidence of superiority of any one membrane tested relative to the others nor any proof that losses were due to irreversible adsorption. However, since losses tended to be highest for fresh membranes, it does appear that irreversible adsorption does occur and that it is

strongest on fresh surfaces. It was also noted that older membranes gave more erratic retardation behavior, and we believe this resulted from nonuniform adsorption and consequent nonuniformity of cross flow.

*Reproducibility and Membrane Stability*

It is still too early to make definitive statements in this area as protein–membrane interactions tend to be very complex. We therefore limit ourselves to selected representative operations.

First it may be noted that the UM2 membrane, from which the data of Figs. 9–11 were obtained, appeared to be quite stable. For example, there is little difference in $R$ between the early runs, represented by circles in Fig. 9, and the late ones, represented by triangles. The later runs did, however, show somewhat greater dispersion.

For the PM5 membrane, however, observed retardation differed increasingly from prediction with increased use. As another indication of membrane fouling, protein losses were normally highest with fresh membranes.

All results are, however, clouded by severe corrosion of the aluminum cell frame, occasioned from the unforeseen use of chloride ion in the buffer solutions. It is likely that this caused fouling and flow maldistribution in both the membranes and porous backing plates. We are preparing to use a redesigned cell.

Finally, one cannot exclude the possibility that adsorption is taking place on the unprotected upstream porous plate.

*Fractionation of Dextrans*

Preliminary tests indicated that polydisperse dextrans, T40 and T500, can be fractionated successfully by UPC. However, there is a definite need for more systematic studies with narrower fractions, and this is planned.

## CONCLUDING REMARKS

### Theory

Experimental evidence, as well as the experience of previous investigators (*11*), suggests that the two-parameter theoretical model, Eq. (34), is adequate for exploratory and preliminary design purposes. Furthermore, transients are of secondary importance under the experimental conditions used. Finally, Eqs. (19) through (22) permit extension of the model to description of skewness, which requires one additional parameter corresponding to $\phi_2$, without insuperable mathematical difficulty.

One could proceed to evaluation of additional parameters, but this is probably not advisable. First, it is generally difficult to obtain experimental data sufficiently precise to justify models with more than three parameters (*12*). Second, the approach used here is not efficient for describing the very complex patterns observed (*13*) for small $\tau$.

## Potential

The sensitivity of $R$ to Pé and very small dispersion predicted at Pé $> 10$, coupled with the sensitivity and flexibility of the apparatus, make this a potentially attractive separation technique. Furthermore, the data obtained with monodisperse proteins bear out these predictions to the degree that they were tested.

At the same time the high boundary concentrations required in the prototype apparatus combined with the possibility of severe adsorption suggest caution in using UPC for protein fractionation. It appears much more promising for the fractionation of more stable polymers such as dextrans or petrochemical derivatives.

Only minor design improvements are needed to adapt UPC for analytical fractionation of stable polydisperse polymers, and this appears to be a very promising area for immediate development.

There is also a distinct possibility that UPC will prove useful for polymer fractionation on a commercial scale, but evaluation of this possibility will require considerable effort.



## REFERENCES


1. M. Bier, *Electrophoresis*, Academic, New York, 1959.
2. K. Clusius and G. Dickel, *Naturwissenshaften*, *27*, 148 (1939).
3. J. G. Kirkwood, "A Suggested Method of Fractionation of Proteins by Electrophoresis Convection," *J. Chem. Phys.* *9*, 878 (1941).
4. L. E. Nielsen and J. G. Kirkwood, "The Fractionation of Proteins by Electrophoresis-Convection," *J. Am. Chem. Soc.*, *68*, 181 (1946).
5. K. D. Caldwell, L. F. Kesner, and J. C. Giddings, "Electrical Field-Flow Fractionation of Proteins," *Science*, *176*, 296 (1972).
6. H. L. Lee, J. F. G. Reis, J. Dohner, and E. N. Lightfoot, "Single-Phase Chromatography: Solute Retardation by Ultrafiltration and Electrophoresis," *AIChE J.*, *20*, 776 (1974).
7. J. C. Giddings, *Dynamics of Chromatography*, Dekker, New York, 1965.
8. J. C. Giddings, "Nonequilibrium Theory of Field-Flow Fractionation," *J. Chem. Phys.*, *49*(1), 81 (1968).
9. J. F. G. Reis, E. N. Lightfoot, and H. L. Lee, "Concentration Profiles in Free-Flow Electrophoresis," *AIChE J.*, *20*, 362 (1974).

10. C. Tanford, *The Physical Chemistry of Macromolecules*, Wiley, New York, 1961.
11. W. N. Gill and R. Sankarasubramanian, "Exact Analysis of Unsteady Diffusion," *Proc. R. Soc. London, Ser. A, 316*, 341 (1970).
12. J. B. Bassingthwaighte, "Blood Flow and Diffusion in Mammalian Organs," *Science, 167*, 1347 (1970).
13. J. F. G. Reis et al., manuscript in preparation.
14. J. F. G. Reis and E. N. Lightfoot, "Electropolarization Chromatography," submitted to *AIChE J.* for publication.

*Received by editor January 28, 1976*